Title
Extended fast-ion D-alpha diagnostic on DIII-Da)

Journal
Review of Scientific Instruments, 81(10)

ISSN
0034-6748

Authors
Muscatello, CM
Heidbrink, WW
Taussig, D
et al.

Publication Date
2010-10-01

DOI
10.1063/1.3475367

Extended fast-ion D-alpha diagnostic on DIII-D[a)]

C. M. Muscatello,[1] W. W. Heidbrink,[1] D. Taussig,[2] and K. H. Burrell[2]
[1]*University of California, Irvine, California 92697, USA*
[2]*General Atomics, San Diego, California 92186, USA*

(Presented 17 May 2010; received 13 May 2010; accepted 3 June 2010; published online 25 October 2010)

A fast-ion deuterium-alpha (FIDA) diagnostic, first commissioned on DIII-D in 2005, relies on Doppler-shifted light from charge-exchange between beam neutrals and energetic ions. The second generation (2G) system was installed on DIII-D in 2009. Its most obvious improvement is the spatial coverage with 11 active in-beam and three passive off-beam views; the latter allows for simultaneous monitoring of the background signal. Providing extended coverage in fast-ion velocity space, the new views possess a more tangential component with respect to the toroidal field compared to their first generation counterparts. Each viewing chord consists of a bundle of three 1.5 mm core fibers to maximize light gathering. For greater throughput, fast f/1.8 optical components are used throughout. The signal is transmitted via fiber optics to a patch panel, so the user is able to choose the detector. FIDA was originally installed with a spectrometer and charge-coupled device (CCD) camera to monitor the full D_α spectrum for two spatial views. 2G adds another spectrometer and CCD that monitor the blue-shifted wing for six spatial views at 1 kHz. In addition, a photomultiplier tube and fast digitizer provide wavelength-integrated signals at 1 MHz for eight spatial views. © *2010 American Institute of Physics.* [doi:10.1063/1.3475367]

I. INTRODUCTION

To achieve burning plasmas in future tokamak reactors, substantial heating power will be required. Neutral beam injection and wave heating at radio frequencies are the two most promising methods. Both mechanisms often produce a non-Gaussian anisotropic suprathermal ion population. The heating efficiency is strongly dependent on how well the energetic ion population deposits its energy to the core bulk plasma. Plasma instabilities can lead to a redistribution or complete loss of fast ions, thereby impairing heating efficiency in the core. Furthermore, an intense population of energetic particles can provide the driving mechanism for some instabilities, which in turn can detrimentally affect the fast ions. Therefore, the need for careful diagnosis of the fast-ion distribution function becomes ever more important as we approach reactor-relevant scenarios.

One such diagnostic method is the fast-ion deuterium-alpha (FIDA) technique.[1,2] It relies on charge-exchange between injected neutral beam particles and the energetic deuterium ions of interest. The first dedicated diagnostic of its kind at DIII-D (Refs. 1 and 3) was installed in 2005 following a test prototype[2] using an existing charge-exchange recombination diagnostic tuned to the D_α wavelength. The first generation version of FIDA will be referred to simply as "FIDA" for the duration of this article. FIDA has been benchmarked against the FIDAsim code that takes into account all relevant atomic physics.[4] Under magnetohydrodynamic-quiescent conditions in low density, L-mode plasmas, FIDA agrees well with classical simulations.[5]

A single FIDA installation provides a measurement of essentially one component of the fast-ion velocity. In velocity space, an ensemble of ion pitches ($V_\parallel/V$) and total energies contribute to the measured signal. An additional installation with a different viewing geometry can measure another component of the velocity; the particles contributing to the signal consist of a different ensemble in velocity space. Due to the success of the original FIDA system and the potential for greater velocity-space and spatial coverage, a new FIDA installation [second generation (2G) FIDA or 2G FIDA] has been commissioned on the DIII-D tokamak.[6] Many design aspects of this new diagnostic were adopted from the existing FIDA system on NSTX.[7] Furthermore, the array of hardware improvements and the addition of a fast-integrated photomultiplier tube (PMT) assembly substantially extend the capabilities of the DIII-D FIDA suite.

II. HARDWARE SETUP

A FIDA diagnostic relies on charge-exchange between injected neutral atoms and energetic deuterium ions. Subsequently, some of the neutralized fast deuterons are in the $n=3$ atomic state. Photons emitted at the Balmer-α wavelength involve the $n=3\rightarrow2$ atomic transition. In the deuteron rest frame, the wavelength lies in the visible spectrum at 656.1 nm. However, due to their suprathermal velocities, the excited fast deuterons impart a Doppler shift to the emitted photon. Consequently, the Balmer-α, or D_α in the case of deuterium, spectral line is modified with a broad low-intensity feature in the presence of a fast deuterium popula-

[a)]Contributed paper, published as part of the Proceedings of the 18th Topical Conference on High-Temperature Plasma Diagnostics, Wildwood, New Jersey, May 2010.

TABLE I. Fiber optic specifications.

Collection fibers	Core material	Numerical aperture	Core diameter	Maximum transmission	Attenuation
11 active chords 3 passive chords	Silica	0.37	1500 μm	>99.8% at 650 nm	3 dB/km at 650 nm

tion. This broad feature, consisting of blue- and red-shifted wings about the D_α line, is the subject of investigation for FIDA.

Collection of visible photons is straightforward using standard optical components. On the tokamak end of the diagnostic, a total of 42 fiber optics make up the viewing chord array. See Table I for the fiber optic specifications. Each radial chord consists of three toroidally displaced fiber views to increase the system's light gathering ability. When a chord is backlit and projected on the midplane, the three spots are toroidally aligned with adjacent spots separated by 10 cm center-to-center. The average spot diameter is ~4 cm, which is approximately twice the intrinsic spatial resolution due to the lifetime of the n=3 atomic state.[8] See Fig. 1 for a comparison of the geometries of the new and old views. Their distinct sightline geometries and viewed neutral sources provide different weightings in fast-ion velocity space, making it possible to compare the trapped and passing ion populations. The old views intersect the magnetic field nearly perpendicularly, having a large vertical component and much smaller toroidal and radial components. These chords utilize one of DIII-D's "cosources" which injects in the same direction as the plasma current in a typical discharge. This geometry prevents contaminating light due to beam emission from entering the collection optics. The new views intersect the field more tangentially, possessing a large vertical and toroidal component. These chords view a neutral beam source which injects in the opposite direction of the typical plasma current on DIII-D; this is a so-called "countersource."

When viewing the beam from behind, the light from beam emission is red-shifted. Therefore, we only concern ourselves with the blue wing of the spectrum, since it is not

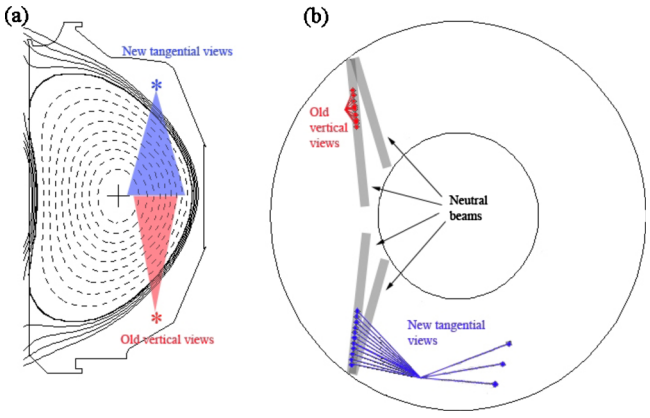

FIG. 1. (Color online) (a) Elevation of DIII-D showing poloidal projection of new and old FIDA viewing chords. (b) Plan view of DIII-D showing toroidal projection of new and old FIDA viewing chords.

complicated by Stark components of the beam emission. The active signals (those viewing a neutral beam) consist of 11 chords spanning major radii of 173–226 cm (normalized toroidal flux coordinate ρ=0.04–0.80, typically). The passive signals (viewing no neutral beam and projecting onto a similar part of the tokamak floor) consist of three chords spanning major radii of 173–211 cm. The difference between an active and passive signal yields the desired net FIDA signal.[1] FIDA utilizes beam modulation to obtain active and passive signals during steady-state periods. 2G FIDA also employs this method of background subtraction, but the three passive views permit an additional level of background monitoring. Each method has its obvious pros and cons: obtaining passive and active signals using beam modulation ensures toroidal equivalence but requires temporal constancy; the active/passive view method ensures temporal equivalence but requires toroidal symmetry.

D-alpha light enters the 2G FIDA collection lens after the rays reflect off a series of mirrors. The purpose of the mirrors is twofold: (1) to redirect the oblique chords through a vertical port in the tokamak and (2) to accommodate both active and passive chords with the same set of optics. The mirrors are ground to 65 nm roughness and 3 μm flatness and are coated for high reflectivity. After their last reflection, the rays pass vertically through an aperture and sapphire window separating the collection lens from vacuum. The lens is a 40 mm diameter, 60 mm focal length Edmund Optics biconvex with antireflective coating yielding maximum transmission at ~650 nm. A lens aperture is fitted to match the fiber optics' numerical aperture of 0.37. The lens focuses all 42 viewing lines onto a fiber optic array. A fiber optic mount is located at the lens's axial focal plane. Many chords have off-axis and oblique incidence as they pass through the lens resulting in a nonplanar focal surface. Because of the spherical nature of the lens, the effect is an approximately spherical focal surface. To account for this, the surface of the fiber optic array was empirically fitted to the lens's focal surface; its radius is ~30 mm.

The light traverses about 50 m of fiber optics and is transmitted to the FIDA diagnostics laboratory. The fibers are arranged onto a patch panel allowing the user to choose which signals should be sent to each instrument. Three instruments are currently available: (1) FIDA; Czerny-Turner spectrometer and charged-coupled device (CCD) camera, (2) s-FIDA; transmission grating spectrometer and CCD camera, and (3) f-FIDA; fast integrating system with PMT.[7] The remainder of this article will focus on the s- and f-FIDA instruments.

A. s-FIDA

Similar to FIDA, s-FIDA is a spectroscopic system with the goal of obtaining the D_α spectrum for several chords. See Table II. The s-FIDA instrument is capable of recording data from 6 chords in a single discharge. A repeat shot is necessary to obtain the entire spatial range. The HoloSpec transmission grating spectrometer[9] is a very compact device with stigmatic imaging; when used in conjunction with our Newport bandpass filter,[10] the spectrometer can employ close positioning of fibers at the input focal plane with low crosstalk

TABLE II. 2G FIDA detector specifications.

	Sampling rate (kHz)	Center λ (nm)	Bandwidth (nm)	Spectral resolution
s-FIDA 6 chords	1	651.5	5	0.5 nm
f-FIDA 8 chords	200 effectively	653	3	NA

among neighboring chords. Three fibers composing a radial chord are stacked vertically with two channels vertically adjacent and three channels arranged horizontally. Because of the short focal length of its lenses, the spectrometer produces strong curvature at the output focal plane.[11] To correct for this curvature, instead of straight input slits, they are designed as arcs of a circle according to Eq. 12 of Ref. 11. Since the dispersion varies strongly across the transverse axis of the spectrometer, varying slit widths are chosen to keep the spectral (energy) resolution constant at ~0.5 nm (~10 keV). Stark splitting from motional $\mathbf{v}\times\mathbf{B}$ and from plasma electric fields causes ~1 nm spread of the D_α emission, so spectral resolutions up to 1 nm are acceptable for a FIDA diagnostic. A Sarnoff CAM1M100 CCD camera[12] captures the spectra on a 1024×1024 pixel chip. Since the vertical pixels for each viewing channel are redundant, they are binned to achieve a readout rate of 1 kHz. Neutrons and gamma rays escape the plasma and can produce contaminant hits on the CCD chip, so the diagnostic must be shielded from such radiation. The shield consists of two walls: the outer wall is a 10 cm thick wall of high-Z 5% borated polyethylene to prevent neutron penetration and it surrounds a 10 cm thick wall of lead to block gamma rays. This design is highly successful and is utilized at DIII-D with most radiation-sensitive detectors.

Both random and systematic errors contribute to uncertainties in an s-FIDA measurement. The three dominant sources of random errors are readout noise, dark current noise, and photon noise. To reduce the effects of dark current, the CCD is cooled to 275 K via a chilled water line and thermoelectric controller (TEC). Lowering the control temperature of the TEC by a few more degrees can further reduce the thermal noise. For a given frame, the thermal noise dominates in the high-energy portion of the spectrum. Photon noise, on the other hand, dominates in the low-energy region, increasing as (number of photon counts)$^{1/2}$. Overall, the signal-to-noise ratio (SNR) is better than unity for all relevant wavelengths except near the injection energy, typically corresponding to $E_\lambda=80$ keV ($\lambda=650$ nm).

B. f-FIDA

When time-averaged during steady conditions, s-FIDA provides the capability to reasonably infer the energy distribution of fast deuterium ions. If a high-resolution time history of the FIDA signal is desired, the s-FIDA system described above will not suffice. Many instabilities such as Alfvén eigenmodes occur at frequencies O(100 kHz), which requires a diagnostic acquisition rate of at least twice that frequency to resolve the fluctuation. Because of its relatively low gain and the requirement to build charge to produce a sufficient SNR, CCDs are insufficiently "fast" acquisition

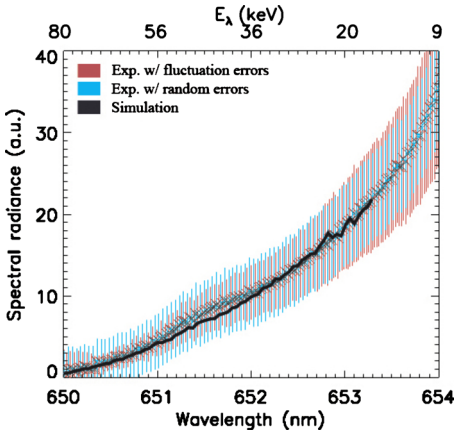

FIG. 2. (Color online) Comparison of time-averaged net FIDA spectra and simulated spectra at $\rho=0.30$. E_λ denotes the fast-ion energy component measured along the sightline of the detector.

devices. Instead, the combined use of bandpass filtering and a PMT can satisfy this need. The goal of f-FIDA is to obtain wavelength-integrated signals on a timescale short enough to resolve high frequency macroscopic fluctuations. See Table II for specifications of the f-FIDA system. It is a compact design and has the capacity for accommodating signals from eight radial chords. The eight fiber bundles are mounted within a 5 cm diameter circle in order to collectively transmit the light signals through a single filter. An array of eight aspheric lenses is positioned away from the fiber bundle by a distance equal to the lens's focal length; they collimate the light for transmission through a bandpass filter centered at 653 nm. Rays oblique to the surface of the filter cause a down-shift in the wavelength pass-band, and the amount of shift depends on the characteristics of the filter. Therefore, a high degree of collimation is required to achieve the designed pass-band. The maximum divergence of the collimated rays is ~2° resulting in a wavelength shift of ~0.2 nm, much smaller than the 3 nm bandwidth. After the light is filtered, the rays are refocused by another array of lenses, and the filtered signal is transmitted to the Hamamatsu H8711-20 PMT (Ref. 13) by a set of jumper fibers. The multichannel PMT is designed as a 4×4 array, and the fibers are arranged in a checkerboard configuration so no two active channels are directly adjacent. This design reduces the electronic and photonic crosstalk by about 10%. To prevent stray light from entering the f-FIDA optics and contaminating the signals, a light-tight aluminum enclosure shields the diagnostic. Each active channel of the PMT generates a current signal, which is first amplified and then sent to a digitizer. Although the digitizer acquires at a 1 MHz sampling rate, the diagnostic can resolve fluctuations up to ~200 kHz. The upper bound of the bandwidth is limited by the number of photons; empirically, the SNR quickly approaches unity for fluctuations above 200 kHz.

III. SAMPLE DATA

Figure 2 displays sample s-FIDA data from a shot during an MHD-quiescent period in L-mode. The plasma current (Ip), toroidal field (Bt), and electron density (n_e) are 0.6 MA, 2 T, and 2.4×10^{13} cm^{-3}, respectively. The experimental

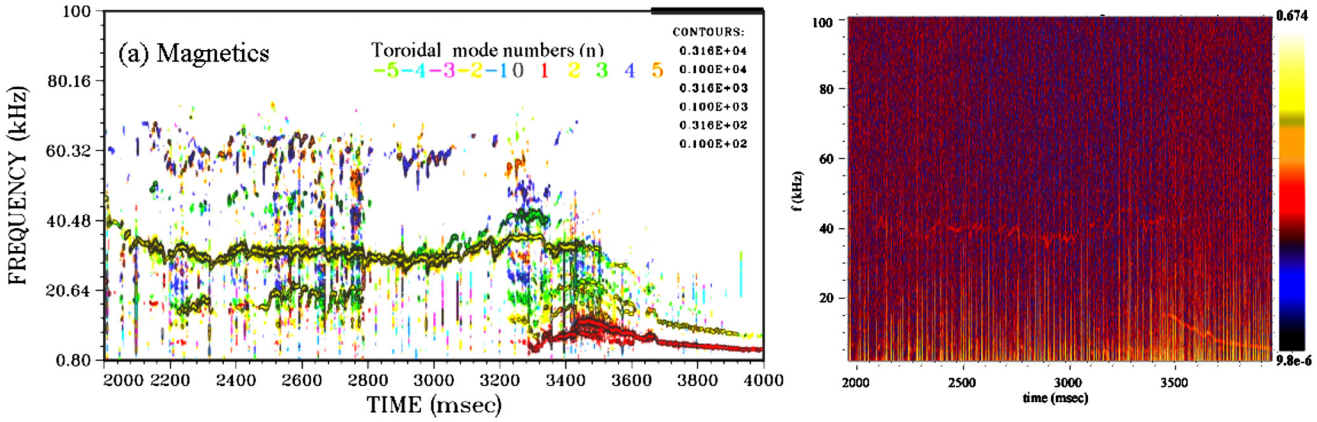

FIG. 3. (Color online) (a) Spectrogram of crosspower between two magnetic probes. Colors indicate toroidal mode number (n). (b) Spectrogram of autopower of f-FIDA chord at ρ=0.15.

FIDA spectrum in Fig. 2 is obtained during neutral beam modulation by averaging many active (beam on) and passive (beam off) spectra over steady conditions of about two fast-ion slowing-down times. The difference between the average *active* spectrum and the average *passive* spectrum results in the *net* FIDA spectrum. The red error bars are calculated by finding the ensemble standard deviation of the averaged spectra. This is the fluctuation error associated with deviations of the experimental spectrum about the mean. The blue error bars are calculated by considering all relevant sources of random noise, i.e., photon, dark, and readout noise. These contribute to the random error associated with counting statistics and random fluctuations in the diagnostic. Evidently, the sizes of the two types of error are comparable. The black curve is a simulated spectrum using the FIDAsim code. At the time of writing, absolute intensity calibrations are not yet available, and the simulated spectrum is normalized to the experimental spectrum. Although no comparison can be made regarding the spectral magnitudes, the spectral shapes are in excellent agreement. Imperfect background subtraction results in a deviation of the experimental spectrum from the simulation around 651–652 nm, corresponding to a CII spectral line.

Figure 3 shows sample data from an H-mode discharge with Ip$\sim$0.8 MA, Bt$\sim$2 T, and n_e ranging at 4–6 $\times 10^{13}$ cm^{-3}. The experiment required $\sim$15 MW of neutral beam power to strike low toroidal mode number (n) neoclassical tearing modes (NTMs). Figure 3(a) is a spectrogram of the crosspower between two magnetic probes separated toroidally by 33°. During this time window, presumably a 3/2 NTM persists until $\sim$3.2 s when it becomes dominantly a 2/1 mode. Figure 3(b) is a spectrogram of the autopower of an active f-FIDA signal from ρ=0.15. There is an obvious coherence in the signal, following the same frequency evolution as the dominant mode; the passive view at the equivalent ρ lacks this feature. Evidently, fast ions interact coherently with the rotating island.

The combined use of FIDA and both the s- and f-FIDA instruments provides a powerful tool for diagnosing the fast-deuterium distribution function. Fast-ion velocity-space comparisons and high temporally resolved signals are now possible on the DIII-D tokamak. The diagnostic suite was employed during the 2009–2010 experimental campaign, and future studies will investigate fast-ion transport mechanisms in the presence of numerous instabilities such as sawteeth, NTMs, fishbones, Alfvén eigenmodes, energetic particle geodesic acoustic modes, drift waves, and microturbulence.

ACKNOWLEDGMENTS

We would like to express our gratitude to M. Podestà, N. Brooks, J. Kulchar, W. Carrig, N. Pablant, and the entire DIII-D Team for their support. This work was supported by U.S. DOE under Grant Nos. SC-G903402 and DE-FC02-04ER54698.

[1] Y. Luo, W. W. Heidbrink, K. H. Burrell, D. H. Kaplan, and P. Gohil, Rev. Sci. Instrum. **78**, 033505 (2007).
[2] W. W. Heidbrink, K. H. Burrell, Y. Luo, N. A. Pablant, and E. Ruskov, Plasma Phys. Controlled Fusion **46**, 1855 (2004).
[3] Y. Luo, W. W. Heidbrink, and K. H. Burrell, Rev. Sci. Instrum. **75**, 3468 (2004).
[4] W. W. Heidbrink, D. Liu, Y. Luo, E. Ruskov, and B. Geiger, Comm. Comp. Phys. (to be published).
[5] Y. Luo, W. W. Heidbrink, K. H. Burrell, E. Ruskov, and W. M. Solomon, Phys. Plasmas **14**, 112503 (2007).
[6] W. W. Heidbrink, Y. Luo, C. M. Muscatello, Y. Zhu, and K. H. Burrell, Rev. Sci. Instrum. **79**, 10E520 (2008).
[7] M. Podestà, W. W. Heidbrink, R. E. Bell, and R. Feder, Rev. Sci. Instrum. **79**, 10E521 (2008).
[8] W. W. Heidbrink, Rev. Sci. Instrum. **81**, 10D727 (2010).
[9] Kaiser Optical Systems, Inc., Ann Arbor, MI, http://www.kosi.com.
[10] Newport Corporation, Irvine, CA, http://www.newport.com.
[11] R. E. Bell, Rev. Sci. Instrum. **75**, 4158 (2004).
[12] Sarnoff Corporation, Princeton, NJ, http://www.sarnoff.com.
[13] Hamamatsu Photonics, Bridgewater, NJ, http://www.hamamatsu.com.